

Optimizing Irrigation Efficiency using Deep Reinforcement Learning in the Field

Xianzhong Ding

University of California, Merced
xding5@ucmerced.edu

Wan Du

University of California, Merced
wdu3@ucmerced.edu

ABSTRACT

Agricultural irrigation is a significant contributor to freshwater consumption. However, the current irrigation systems used in the field are not efficient. They rely mainly on soil moisture sensors and the experience of growers, but do not account for future soil moisture loss. Predicting soil moisture loss is challenging because it is influenced by numerous factors, including soil texture, weather conditions, and plant characteristics.

This paper proposes a solution to improve irrigation efficiency, which is called DRLIC. DRLIC is a sophisticated irrigation system that uses deep reinforcement learning (DRL) to optimize its performance. The system employs a neural network, known as the DRL control agent, which learns an optimal control policy that considers both the current soil moisture measurement and the future soil moisture loss. We introduce an irrigation reward function that enables our control agent to learn from previous experiences. However, there may be instances where the output of our DRL control agent is unsafe, such as irrigating too much or too little water. To avoid damaging the health of the plants, we implement a safety mechanism that employs a soil moisture predictor to estimate the performance of each action. If the predicted outcome is deemed unsafe, we perform a relatively-conservative action instead. To demonstrate the real-world application of our approach, we developed an irrigation system that comprises sprinklers, sensing and control nodes, and a wireless network.

We evaluate the performance of DRLIC by deploying it in a testbed consisting of six almond trees. During a 15-day in-field experiment, we compared the water consumption of DRLIC with a widely-used irrigation scheme. Our results indicate that DRLIC outperformed the traditional irrigation method by achieving a water savings of up to 9.52%.

1 INTRODUCTION

Agriculture is a major contributor to the consumption of ground and surface water in the United States, with estimates suggesting that it accounts for approximately 80% of the Nation's water use, and over 90% in many Western states¹. Specifically, California's almond acreage in 2019 was estimated at 1,530,000 acres, and almond irrigation alone is estimated to consume roughly 195.26 billion gallons of water annually [4, 5]. Given the current drought affecting many Western states, it is critical to improve irrigation efficiency to conserve our limited freshwater reserves. This study focuses on enhancing the irrigation efficiency of almond orchards.

The primary objective of agricultural irrigation is to maintain the health of trees and maximize crop production. Achieving this goal requires maintaining the soil moisture of the trees within

a specific range, typically between the Field Capacity (FC) level and the Management Allowable Depletion (MAD) level. If the soil moisture falls below the MAD level, almond trees may experience discoloration or even die. Conversely, if the soil moisture exceeds the FC level, it can lead to reduced oxygen movement in the soil, negatively impacting the tree's ability to absorb water and nutrients. Both FC and MAD levels are dependent on the soil type and plant species. Therefore, to determine the appropriate FC and MAD levels for a specific orchard, it is essential to identify the soil type and refer to a manual that outlines the corresponding FC and MAD levels for that soil type [6].

To ensure that the soil moisture remains within the MAD and FC range, the sprinklers must be activated every day or every few days, depending on the soil moisture level. Given the high evaporation rate in California, daily irrigation is recommended by the Almond Board of California [6] and is used in many existing irrigation systems [7, 8]. In most micro-sprinkler irrigation systems, irrigation is performed at night to reduce water loss due to evaporation, which can be as high as 14-19% during the day [9]. The irrigation scheduling problem involves determining the appropriate amount of water to be applied to each sprinkler to ensure that the soil moisture remains within the MAD and FC range until the next irrigation cycle. This decision is based on the current soil moisture level and the predicted soil moisture loss for the following day, which is influenced by factors such as soil type, local weather conditions, and plant properties (e.g., root length and leaf number). The objective of irrigation is to provide trees with an appropriate amount of water such that the soil moisture remains above the MAD level until the next irrigation cycle.

Developing optimal irrigation control strategies requires accurate soil moisture loss prediction models. Traditional Model Predictive Control (MPC) methods can be utilized for optimal irrigation control if such a prediction model exists, but the accuracy of the model can have a significant impact on the performance of these methods [10, 11]. Obtaining an accurate soil moisture prediction model for an almond orchard is challenging, as soil moisture is influenced by multiple factors, including soil type, topography, ambient temperature, humidity, solar radiation intensity, and plant transpiration [12]. Additionally, customized soil moisture models must be developed for each orchard, limiting the scalability of MPC-based approaches. These two limitations have prevented the use of MPC-based methods in orchards.

The irrigation systems currently used in orchards are ET-based or sensor-based control methods. Evapotranspiration (ET) is an estimate of moisture lost from soil, subject to weather factors such as wind, temperature, humidity, and solar irradiance. All these weather factors are being measured by weather stations. Local ET value is also publicly available [13] and updated every hour. Based

¹Irrigation and Water Use: <https://www.ers.usda.gov/>

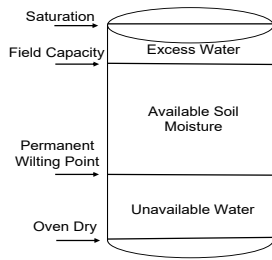


Figure 1: The various levels of the soil water content [1].

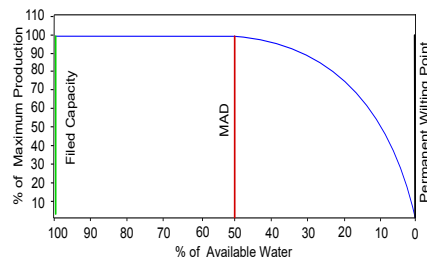


Figure 2: How plant production (growth) is affected by soil water content [2].

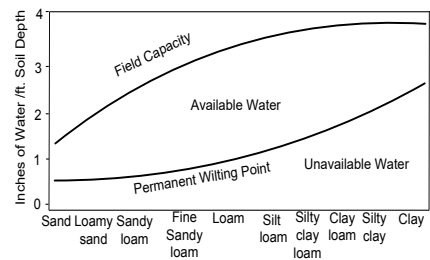


Figure 3: Relationship between available water capacity and soil texture [3].

on the ET values since the last irrigation time, ET-based irrigation controllers start the sprinklers to compensate for the soil moisture loss. However, they do not consider the soil moisture loss of next day before the next irrigation time. If the soil moisture loss in the last day does not equal the soil moisture loss that will happen in the next day, ET-based irrigation may under-irrigate or over-irrigate. In addition, a safe margin of water [14] is normally added, making ET-based methods over-irrigate in most cases [7, 15].

With accurate soil moisture sensors, irrigation controllers can react directly to the soil moisture level [7]. The commonly-used controllers are "rule-based", in which a certain amount of water will be supplied once soil moisture deficiency is detected. However, parameters for the time and the amount to irrigate are generally tuned by growers by their experience. Without predicting how much water will be lost, sensor-based irrigation normally does not systematically take into account future weather information, such as rain and wind in next day.

To solve the limitations of the above existing irrigation schemes, we develop *DRLIC*, a practical Deep Reinforcement Learning (DRL)-based irrigation system, which automatically learns an optimal irrigation control policy by exploring different control actions. In *DRLIC*, a control agent observes the *state* of the environment, and chooses an *action* based on a control policy. After applying the action, the environment transits to a next state and the agent receives a *reward* to its *action*. The goal of learning is to maximize the expected cumulative discounted reward. *DRLIC*'s control agent uses a neural network to learn its control policy. The neural network maps "raw" observations to the irrigation decision for the next day. The state includes the weather information (e.g., ET and Precipitation) of today and next day.

To minimize the irrigation water consumption while not impacting the trees' health, we design a reward function that considers three specific situations. If the soil moisture result is higher than the FC level or lower than the MAD level, we will give the control agent a negative reward. If the soil moisture result is within the MAD and FC range, we will give the control agent a positive reward inversely proportional to the water consumption.

Ideally, *DRLIC*'s control agent should be trained in a real orchard of almond trees. However, due to the long irrigation interval (one day in our case), the control agent can only explore 365 control actions per year. It will take 384 years to train a converged control agent. Therefore, to speed up the training process, we train our control agent in a customized soil-water simulator. The simulator

is calibrated by the 2-month soil moisture data of six almond trees and can generate sufficient training data for *DRLIC* using 10-year weather data.

Working as an irrigation controller in the field, the control agent may meet some states that it has not seen during training, especially for the control agent trained in a simulated environment. In this situation, the control agent may make a poor decision that violates plants' health, i.e., making the soil moisture level lower than the MAD level or higher than the FC level. To handle the gap between the simulated environment and the real orchard, we design a safe irrigation mechanism. If *DRLIC*'s control agent outputs an unwise action, instead of executing that action, we use the ET-based method to generate another action. We use the soil moisture model of our soil-water simulator to verify whether an action is safe or not.

To evaluate the performance of *DRLIC*, we build an irrigation testbed with micro-sprinklers currently used in almond orchards. Six almond trees are planted in two raise-beds. Each tree has a sensing and control node, composed of an independently-controllable micro-sprinkler and a soil moisture measurement set (two sensors deployed at different depths in the soil). Each node can send its sensing data to our server via IEEE 802.15.4 wireless transmission, and receive irrigation commands from the server.

Our testbed has been successfully deployed in the field, where we have collected soil moisture data from six sensing and control nodes for over three months. Using two months of this data, we trained our soil moisture simulator, while 0.5 months of data were used to validate its accuracy. Once we trained the control agent of *DRLIC*, we deployed it in our testbed for 15 days. The results of the experiment showed that *DRLIC* can reduce water usage by 9.52% compared to the ET-based control method, without causing any harm to the health of almond trees

We summarize the main contributions of this paper as follows:

- We design *DRLIC*, an irrigation method that utilizes DRL to save water usage in agriculture.
- A set of techniques have been proposed to transform *DRLIC* into a practical irrigation system, including our customized design of DRL states and reward for optimal irrigation, a validated soil moisture simulator for fast DRL training, and a safe irrigation module.
- We build an irrigation testbed with customized sensing and actuation nodes, and six almond trees.
- Extensive experiments in our testbed show the effectiveness of *DRLIC*.

Table 1: Suggested MAD For Different Crops [2]

Crop	MAD (%)	Crop	MAD (%)
Beans	40	Potatoes	30
Blueberries	50	Raspberries	50
Corn	50	Strawberries	50
Alfalfa	55	Sweet Corn	40
Mint	35	Tree Fruit	50

2 IRRIGATION PROBLEM

Soil Water Content Parameters. Soil plays a critical role in the water supply for plants, serving as a reservoir for their hydration needs. Typically, up to 35% of the space in soil can be filled with water. Soil water content is a measure of the amount of water present in the soil, often expressed as a percentage of water by volume (%) or as inches of water per foot of root (in/ft). Soil moisture sensors are commonly employed to measure the soil water content at a specific location in the soil. For trees with roots that extend several feet, multiple soil moisture sensors may be utilized at various depths along the root structure. The root is typically divided into a defined number of sections, with a soil moisture sensor positioned at the midpoint of each section to enable accurate monitoring of the plant’s hydration levels. The soil water content of the tree can be calculated as $V = \sum_{j=1}^M \varphi_j * d_j$, where M is the number of moisture sensors installed at different depths (M is 2 in our experiments); φ_j is the reading measured by the j th soil moisture sensor; and d_j is the depth that the j th moisture sensor covers. If such a set of soil moisture sensors are used to measure the soil water content of a region, they will be deployed under a typical tree that has similar soil water content with most of the trees in the region.

To ensure the health of a plant, it is essential to ensure that its roots have access to a sufficient supply of water. Figure 1 provides an illustration of two critical soil water content levels that are crucial for plant health [1]. Firstly, the Permanent Wilting Point (PWP) represents the minimum threshold of soil water content below which plants are unable to draw sufficient moisture from the soil. Prolonged periods of soil moisture levels below the PWP can lead to plant wilting or death. Secondly, if the soil water content exceeds the Field Capacity (FC) level, there is an excess of water in the soil, which can lead to water wastage and rotting of the roots over time, ultimately compromising the plant’s health. Therefore, *the goal of irrigation systems is to maintain soil water content between the PWP level and the FC level.*

The primary objective of irrigation for fruit trees like almond is to achieve maximum production. To achieve this goal, it is crucial to maintain soil moisture content above the Management Allowable Depletion (MAD) level instead of the PWP level. As shown in Table 1, the MAD level can vary for different types of crops (e.g., 40% for corn, 50% for fruit trees). Figure 2 illustrates the relationship between soil moisture content and almond tree production [2]. From Figure 2, it can be observed that the MAD level for almond trees is the median value (50%) between the Field Capacity (FC) level and the Permanent Wilting Point (PWP) level. Therefore, *almond trees can achieve their maximum production, as long as we maintain the soil water content above the MAD level.*

How to Determine these Parameters in an Orchard? The Available Water holding Capacity (AWC) of the soil is defined as

the soil water content range between the FC level and the PWP level. Figure 3 shows that AWC varies for different soil types [3]. The texture, presence, and abundance of rock fragments, as well as the depth and layers of soil, can affect the AWC of the soil. Finer-textured soils, such as loam, have a higher AWC than sandier soils [3]. On the other hand, soils with more clay, such as clay loam, have a lower AWC than loamy soils [3].

The AWC of a tree, V_{awc} , can be calculated as $V_{awc} = \sigma_{awc} * D_{foot}$, where σ_{awc} is the soil’s AWC and D_{foot} is the tree’s root depth in the unit of feet. The AWC for different soil types, σ_{awc} , can be found in [3].

The PWP level for a soil type, V_{pwp} , can also be calculated as $V_{pwp} = \varphi_{pwp} * D_{inch}$, where φ_{pwp} is the soil moisture content at the wilting point of that soil type and D_{inch} are the root depth of the plant in the unit of inches. φ_{pwp} for a specific soil type can be found in [3].

Based on the above two parameter (V_{awc} and V_{pwp}), we can also obtain the FC level as $V_{fc} = V_{awc} + V_{pwp}$, and the MAD level as $V_{mad} = \alpha * V_{awc} + V_{pwp}$, where α is set to 50% for almond trees.

How to Use these Parameters for Irrigation? The main objective of irrigation is to maintain the soil water content of plants between the Field Capacity (FC) level and the Management Allowable Depletion (MAD) level. To achieve this goal, it is crucial to determine the soil’s Available Water holding Capacity (AWC) and the Permanent Wilting Point (PWP) level (V_{awc} and V_{pwp}), which depend on the soil type, texture, and layers. Once we identify the soil type, we can calculate these parameters using the methods discussed earlier. However, in large orchards with varying soil types and changing parameters, it is essential to adjust the irrigation system’s setting accordingly.

How Many Valves to Control in an Orchard? Ideally, the sprinkler for each tree should be individually controlled, since the ET of each tree in an orchard varies from 0.12 to 0.20 inches [16]. Moreover, the soil type also varies spatially in an orchard [6], e.g., there are 10 soil type differences with soil clay loam accounting for from 45.6% to 54.7% and 0 to 8 percent slopes in a 60-acre orchard of California². However, there are around 75-125 almond trees in one acre, it is costly to deploy a soil moisture sensor under each tree. Thus, an orchard is normally divided into several irrigation regions based on the similarity of soil texture. A valve is used in each irrigation region to control all the sprinklers. The irrigation problem of a large orchard is to control a number of valves. This paper is focused on irrigation scheduling, but not field partitioning. A simple way to partition an orchard into several irrigation regions is to survey the soil samples across the orchard using an auger. Growers normally conduct the survey for other purposes too, such as planning the density of trees and fertilizing the trees.

3 DRLIC SYSTEM DESIGN

In this section, we first give an overview of DRLIC. We model the irrigation problem as a Markov decision process. We design a DRL-based irrigation scheme and a safe irrigation module.

²Soil Map: <https://casoilresource.lawr.ucdavis.edu/gmap/>

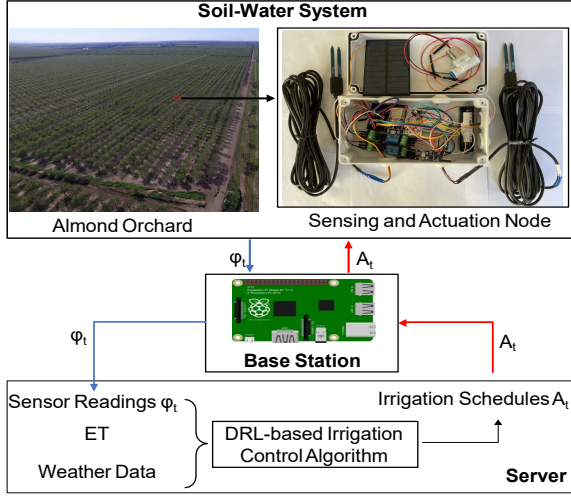


Figure 4: *DRLIC* System Architecture.

3.1 Overview

Figure 4 shows the system architecture of *DRLIC*, which is composed of two key components, i.e., a wireless network of sensing and actuation sprinkler nodes, and a DRL-based control algorithm.

For an almond orchard, we install the sensing and actuation node for each irrigation region. One sensing and actuation node is equipped with a set of soil moisture sensors that are deployed at different depths in the soil. Sensing data is transmitted to the base station via an IEEE 802.15.4 network. The *Base Station* collects the data from *DRLIC* nodes and sends them to a local server using Wi-Fi. These sensing data collected from all *DRLIC* nodes creates a “snapshot” of the soil moisture readings ϕ_t across the entire orchard.

On the server, the DRL-based irrigation control agent makes irrigation decisions based on the soil moisture sensors’ readings, ET and weather data from local weather stations. It provides the optimal irrigation schedule for all *DRLIC* nodes. The objective of *DRLIC* is to minimize the total irrigation water consumption while meeting the requirement of almond health. The server will send the generated irrigation schedules A_t to all *DRLIC* nodes. By receiving a command, a node may open its sprinkler by a latching solenoid with two relays. The implementation details of the nodes will be introduced in Section 4.

3.2 MDP and DRL for Irrigation

We adopt the daily irrigation scheme, i.e., the irrigation starts at 11 PM every day. Each time, the controller decides how long to open each sprinkler to guarantee that the soil water content will be still within the MAD and FC range tomorrow night. The future soil water content is determined by the current soil water content, the irrigated water volume, the trees’ water absorption, and soil water loss (caused by runoff, percolation and ET). Such a sequential decision-making problem can be formulated as a Markov Decision Process (MDP), modeled as $\langle S, A, T, R \rangle$, where

- S is a finite set of states, which includes sensed moisture level from orchard and weather data from local station.
- A is a finite set of irrigation actions for all control valves.

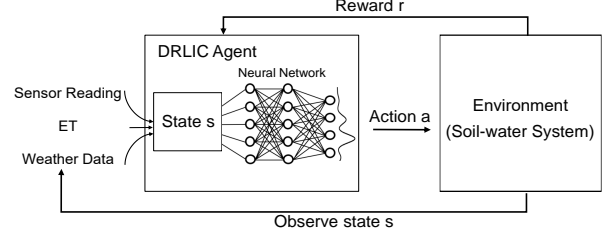


Figure 5: Deep Reinforcement Learning in *DRLIC*.

- T is the state transition function defined as $T: S \times A \rightarrow S$. The soil water content at next time step is determined by current soil water content and the irrigation action.
- R is the reward function defined as $S \times A \rightarrow \mathbb{R}$, which qualifies the performance of a control action.

Based on the above MDP-based irrigation problem formulation, we will find an optimal control policy $\pi(s)^*: S \rightarrow A$, which maximizes the accumulative reward R . We cannot apply conventional tools (e.g., dynamic programming) to search for the optimal control policy, because the state transition function is hard to analytically characterize. In this paper, we consider an RL-based approach to generating irrigation control algorithms. Unlike previous approaches that use pre-defined rules in heuristic algorithms, our approach will learn an irrigation policy from observations.

DRL is a data-driven learning method. It has been widely applied in many control applications [17–22]. DRL learns an optimal control policy through interacting with the environment. At each time step t , the control agent selects an action $A_t = a$, given the current state $S_t = s$, based on its policy π_θ .

$$a \sim \pi_\theta(a|s) = \mathbb{P}(A_t|S_t = s; \theta) \quad (1)$$

In DRL, the control policy is approximated by a neural network parameterized by θ [23]. When the control agent takes the action a , a state transition $S_{t+1} = s'$ occurs based the system dynamics f_θ (Equation 2), and the control agent receives a reward $R_{t+1} = r$.

$$s' \sim f_\theta(s, a) = \mathbb{P}(S_{t+1}|S_t = s, A_t = a) \quad (2)$$

$$\theta^* = \underset{\theta}{\operatorname{argmax}} \mathbb{E}_{\pi_\theta} [r] \quad (3)$$

Due to the Markov property, both reward and state transition depend only on the previous state. DRL then finds a policy π_θ that maximizes the expected reward (Equation 3).

Why do we use DRL for irrigation control?

- DRL learns an optimal irrigation control policy directly from data, without using any pre-programmed control rules or explicit assumptions about the soil-water environment.
- DRL allows us to use domain knowledge to train an irrigation control agent (a neural network) without labeled data.
- The generalization ability of the neural network enables the control agent to better handle the dynamically-varying weather and ET data.

3.3 Deep Reinforcement Learning in *DRLIC*

Figure 5 summarizes the DRL architecture of *DRLIC*. The irrigation control policy (*DRLIC* Agent) is derived from training a neural

network. The agent takes a set of information as input, including current soil water content, today’s weather data (e.g., ET and precipitation), and the predicted weather data for tomorrow. Based on the input, the agent outputs the best action, i.e., the amount of water to irrigate. Until the next day at 11 PM, the resulting soil water content is observed and passed back to the agent to calculate a reward. The agent uses the reward to update the parameters of the neural network for better irrigation control performance. Next, we introduce the design of each DRLIC component.

3.3.1 State in DRLIC. The state in our irrigation MDP model contains the information of three parts. (a) Sensed state, which is the soil water content measured by DRLIC nodes. (b) Weather-related state, which includes the current and predicted state variables from weather station. (c) Time-related state, which is about date information.

Sensed State. The soil water content of each irrigation region can be determined through the use of Equation 6, which takes into account the sensor readings φ obtained from the DRLIC node.

Weather-related State. It is a vector containing the weather information of current day and next day: ET (inch), Precipitation (inch), maximum, average, minimum Temperature ($^{\circ}$ F), maximum, average, minimum Humidity (%), average Solar Radiation (Ly/day), average Wind Speed (mph), Predicted ET by Equation 16 (inch), and forecasted Precipitation (inch) from local weather station.

Time-related State. Date including the month. There are several states that can change over time, including the water requirements of plants and the weather-related state introduced above. Plant water requirements vary by growth stage, and weather conditions change with the seasons.

3.3.2 Action in DRLIC. Based on the current state outlined above, our irrigation scheduling is to find the best amount of water to irrigate (inch), which can maintain plant health (or maximize production) with minimum water consumption. The action is a vector that contains the water amount to irrigate for each irrigation region in an orchard. When the agent outputs an action, we will convert the amount of irrigation water to the open time duration (td) td_i for i th micro-sprinkler. It is calculated as $td_i = a_i/I$, where I is the irrigation rate. We set I to 0.018 inch/min according to the specifications of the micro-sprinklers used in our testbed.

3.3.3 Reward in DRLIC. We define the reward function to express our objective of achieving good plant health with minimum water consumption. Both plant health and water consumption should be incorporated in the reward function. As we know from Section 2, to achieve the maximum production of almond trees, we need to maintain the soil water content between the MAD level and FC level. We use the soil water content deviation from these two levels as a proxy for plant health.

To minimize water consumption while not affecting the plant health, we consider three situations in the design of the reward, as shown in Equation 5. First, when the soil water content (V_i) for i th irrigation region is higher than the FC (V_{fc}) level, the irrigated water is more than the plants’ need. In this case, the plants’ health is affected by over-irrigated water, and water consumption is too high. Second, when V_i is between V_{fc} and V_{mad} , the plants are in good health. In this case, we strive to maintain the V_i close to V_{mad}

Table 2: Parameter Setting in Reward.

Parameter	Value	Parameter	Value
λ_1	3	α	50 (%)
μ_1	8	D_{inch}, D_{foot}	23.62 inches, 1.97 (feet)
μ_2	3	d	11.81 (inches)
λ_3	10	φ_{pwp}	10 (%)
μ_3	1	σ_{awc}	2.4 (in./ft.)

to save water, so we give a reward inversely proportional to the water consumption. Third, when V_i is lower than V_{mad} , the plants are under water stress. The plants’ health is significantly impacted, proportional to the distance between V_i and V_{mad} .

By considering the above three situations, our reward function is defined as follows:

$$R = - \sum_{i=1}^N R_i \quad (4)$$

$$R_i = \begin{cases} \lambda_1 * (V_i - V_{fc}) + \mu_1 * a_i, & V_i > V_{fc} \\ \mu_2 * a_i, & V_{fc} > V_i > V_{mad} \\ \lambda_3 * (V_{mad} - V_i) + \mu_3 * a_i, & V_i < V_{mad} \end{cases} \quad (5)$$

$$V = \sum_{j=1}^M \varphi_j * d_j \quad (6)$$

$$V_{mad} = \alpha * V_{awc} + V_{pwp} \quad (7)$$

$$V_{fc} = V_{awc} + V_{pwp} \quad (8)$$

$$V_{pwp} = \varphi_{pwp} * D_{inch} \quad (9)$$

$$V_{awc} = \sigma_{awc} * D_{foot} \quad (10)$$

where N is the number of irrigation regions in one orchard. a is the amount of water from the RL agent. σ_{awc} and φ_{pwp} are set by referring to the manual of California Almond Board [6] based on our specific soil type in our testbed. Equations 6, 7, 8, 9 and 10 have been introduced in Section 2.

In our current implementation, the parameters of our reward function are set to the values shown in Table 2, based on the specifications of our testbed. The parameters in Equation 5 (i.e., λ_1 , μ_1 , μ_2 , λ_3 and μ_3) are set to the best values that provide the best rewards during training. Their values are set by grid search, which will be introduced in detail in Section 5. The values of these parameters in Table 2 confirm with our design goal of the reward function. First, when V_i is larger than V_{fc} , we give penalties due to both plants’ health and water consumption ($\lambda_1 = 3$, but $\mu_1 = 8$). Second, when V_i is lower than V_{mad} , we give a higher penalty due to plants’ health ($\lambda_3 = 10$, but $\mu_3 = 1$).

3.4 DRLIC Training

3.4.1 Policy Gradient Optimization. In the above DRL framework, a variety of policy gradient algorithms can be used to train the irrigation control agent. Policy gradient algorithms achieve the objective in Equation 3 by computing an estimate of the policy gradient and optimizing the objective through stochastic gradient ascent (Equation 11).

$$\theta \leftarrow \theta + \alpha \nabla_{\theta} \mathbb{E}_{\pi_{\theta}} [r] \quad (11)$$

In this work, we use proximal policy optimization (PPO) [24], which has been successfully applied in many applications such as navigation [25] and games [26]. PPO is known to be stable and robust to hyperparameters and network architectures [24].

PPO minimizes the loss function in Equation 12, which is equivalent to maximizing the Monte Carlo estimate of rewards with regularization. The advantage function \hat{A}_t given by Equation 13 is used to estimate the relative benefit of taking an action from a given state.

$$L_{PPO}(\theta) = -\hat{\mathbb{E}}_t[\min(w_t(\theta)\hat{A}_t, \text{clip}(w_t(\theta), 1 - \epsilon, 1 + \epsilon)\hat{A}_t)] \quad (12)$$

$$\hat{A}_t = \sum_{i=0}^{\infty} \gamma^i r_{t+i} \quad (13)$$

$$w_t(\theta) = \frac{\pi_{\theta}(a_t | s_t)}{\pi_{\theta_{old}}(a_t | s_t)} \quad (14)$$

In Equation 14, $\pi_{\theta}(a_t | s_t)$ is the policy being updated with the loss function and $\pi_{\theta_{old}}(a_t | s_t)$ is the policy that was used to collect data with environment interaction. As the data collection policy differs from the policy being updated, it introduces a distribution shift. The ratio $w_t(\theta)$ corrects for this drift using importance sampling. The ratio of two probabilities can blow up to large numbers and destabilize training, so the ratio is clipped with ϵ .

3.4.2 Data Collection and Preprocessing. On day t , the *DRLIC* agent observes a state s (e.g., moisture level), and then chooses an action (water amount). After applying the action, the soil-water environment's state transits to s_{t+1} next day and the agent receives a reward r . After that, a data pair (s_t, a_t, r_t, s_{t+1}) can be collected. We conduct data normalization by subtracting the mean of the states/action and dividing by the standard deviation. We use 10-year weather data (2010-2020) to generate the data pairs in our dataset, which will be used to train our *DRLIC* agent.

3.4.3 Training Process. Ideally, *DRLIC*'s control agent should be trained in an orchard of almond trees. A well-trained DRL agent needs 384 years to converge due to the long control interval of irrigation systems. It is impossible to train *DRLIC* agent in an orchard. A feasible solution is to refer to a high-fidelity simulator. However, there are no such simulators available in the soil-water domain. Then we decide to leverage a data-driven simulator to speed up the training process. We employ the soil water content predictor introduced in Section 3.5 as our soil-water simulator. The simulator allows *DRLIC* to "experience" the weather of 10 years in several minutes.

The training procedure of *DRLIC* is outlined in Algorithm 1. We train *DRLIC* using 1000 episodes and length of an episode as 30 days. For each episode, we can collect 30 training data pair (s_t, a_t, r_t, s_{t+1}) under different weather data and leverage Equation 12 to optimize the objective in Equation 3 through stochastic gradient ascent. The training ends once Algorithm 1 converges: at the end of each episode the total reward obtained is compared with the previous total. If the current episode reward does not change by $\pm 3\%$, we consider the policy has converged. If the policy does not converge, the training will continue up to a maximum of 100 training iterations (# episodes = 100). After the training, we will deploy the trained *DRLIC* agent into the real almond orchard.

Algorithm 1: *DRLIC* Training Algorithm

Input: State s , Action a , Reward r , an initialized policy, π_{θ} ;
Output: A trained irrigation control agent ;

- 1 **for** $i = 0, \dots, \# \text{ Episodes}$ **do**
- 2 $State \leftarrow Soil - waterenvironment$;
- 3 $\theta_{old} \leftarrow \theta$;
- 4 **for** $t = 0, \dots, \# \text{ Steps}$ **do**
- 5 $\hat{a}_t = \pi_{\theta}(s_t)$;
- 6 $s_{t+1}, r_{t+1} = env.step(\hat{a}_t)$;
- 7 Compute \hat{A}_t ;
- 8 With minibatch of size M ;
- 9 $\theta \leftarrow \theta - \alpha \nabla_{\theta} L_{PPO}(\theta)$;

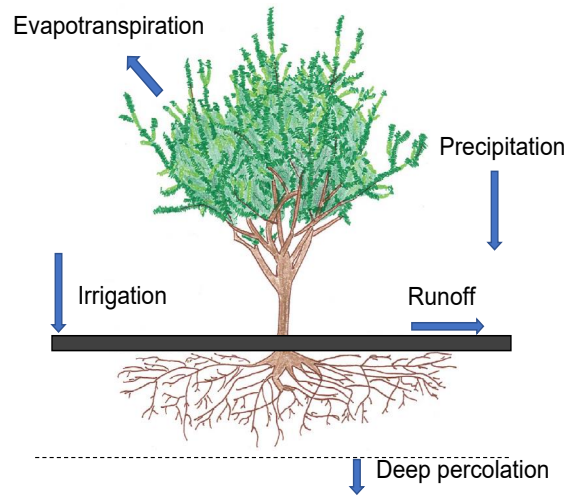


Figure 6: Water Balance in the Root Zone Soil.

When we are given a new environment (e.g., a new orchard), we first need to collect the real-world irrigation data of new environment by existing controller (e.g., ET-based control) to build a soil water content predictor to describe the water balance in the root zone soil. Then we leverage the soil water content predictor to speed up the training process, after that, we deploy the well-trained *DRLIC* agent for this new orchard.

3.5 Safe Mechanism for Irrigation

We design a safe mechanism that integrates the RL and ET controller in a coupled close-loop. Figure 7 illustrates the workflow of safe mechanism, with the following key elements. (i) Different from the pure RL framework, we introduce a safety moisture condition detector to evaluate whether the RL algorithm outputs a safe action. (ii) If so, the action goes to the RL agent, who will be in charge of irrigation control. (iii) Otherwise, we will use an ET-based controller to generate an action for that control cycle. (iv) *DRLIC* will the RL agent for the future control cycles. We now introduce the soil water content predictor and safety condition detector.

Soil Water Content Predictor. To enable early detection of an unsafe action, we design a soil water content predictor to predict

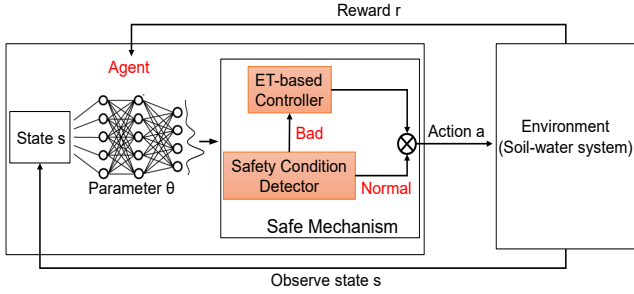


Figure 7: Reinforcement Learning with Safe Mechanism.

Table 3: Coefficients of Predictor for Each Tree.

	c1	c2	c3	b	R ²	NRMSE
Tree1	0.973	0.288	-0.103	0.003	0.982	0.062
Tree2	0.937	0.325	-0.121	0.013	0.985	0.071

the moisture trend after taking an action. Then we design a safe condition detector to detect almond health penalty $p(t)$. The idea is to detect whether the damage metric for an almond tree is higher than a threshold. If so, the detector will command *DRLIC* to switch from RL to ET-based controller.

We design a soil water content predictor to describe the water balance in the root zone soil. As shown in Figure 6, the variations of water storage in the soil are caused by both inflows (irrigation and precipitation) and outflows (evapotranspiration). This leads to the following mathematical expression:

$$V_{i,t+1} = c_1 * V_{i,t} + c_2 * (A_{i,t} + P_t) + c_3 * E_t + b \quad (15)$$

$$E_t = \Gamma_c * RA * TD^{(1/2)} * (T_t + 17.8^\circ C) \quad (16)$$

where $V_{i,t+1}$ denotes the predicted moisture level in the root zone for i th irrigation region after taking the action from RL, E_t and P_t are the plants' ET and the measured rainfall. In time period t , and $A_{i,t}$ is the irrigation amount for i th irrigation region. c_1 , c_2 , and c_3 are coefficients. It is assumed in this work that runoff and water percolation are proportional to soil moisture level [27–29] in Equation 15. All the coefficients can be determined by means of system identification techniques [30]. All variables are normally expressed in inches.

The weather data can be get from local weather station. For *ET*, we adopt the simple calculation model established in [31]. As shown in Equation 16, where Γ_c is a crop-specific parameter. *RA* stands for extraterrestrial radiation, which is in the same unit as E_t . *TD* denotes the annual average daily temperature difference, which can be derived from local meteorological data, and T_t is the average outdoor temperature during the t th time period.

Safety Condition Detector. We employ the difference between predicted moisture level and lower bound as a detector to estimate the almond tree damage. As explained in Section 2, *MAD* is the lower bound. Then we use $\sum_{i=1}^N (V_{mad} - V_{i,t+1})$ as a safety condition detector, $V_{i,t+1}$ denotes the predicted moisture level from i th irrigation region for t timestep. V_{mad} is the water content lower bound. *DRLIC* will evoke ET-based controller once safety condition detector detects the dangerous irrigation action.



Figure 8: Testbed and Microsprinkler Irrigation System.

Parameter Learning of our Soil Water Content Predictor.

We leverage the designed testbed to collect the irrigation amount of almond trees for 2 months. The ET value for each day is collected from a local weather station [13] and the moisture level for each tree is collected by the designed *DRLIC* node. Then the linear least square method was applied to estimate the coefficients. R^2 is used to explain the strength of the relationship between the moisture level and related factors. Normalized root-mean-square error (NRMSE) is used as a goodness-of-fit measure for predictors. The results are shown in Table 3, we can see that the R^2 is close to 1 indicating that the irrigation, ET and precipitation have a strong relationship with soil water content for the tree. The NRMSE is less than 0.1 which means that the predictor can achieve accurate prediction for soil water content.

4 TESTBED AND HARDWARE

4.1 Testbed and Microsprinkler Description

Figure 8 shows our micro-sprinkler irrigation testbed. The micro-sprinkler irrigation system is installed and designed to be identical in hardware, micro-sprinkler coverage, etc. This irrigation system measures 290 cm x 160 cm, with micro-sprinklers arranged in a 3x2 grid, each 97cm from the next. The micro-sprinklers chosen were 1/4", 360° pattern by Rainbird, which are currently considered state-of-the-art in micro-sprinkler technology. Six all-in-one young almond trees were planted into the testbed (three for each). The average height is 2 meters. The soil with 2.7 m³ volume is collected from a local orchard that is a typical loam soil and the plant-available water-holding capacity is 2.4 inches of water per foot.

4.2 DRLIC Node Development.

The designed *DRLIC* node in Figure 4 consists of four main parts: sensors, actuator, power supply and transmission module.

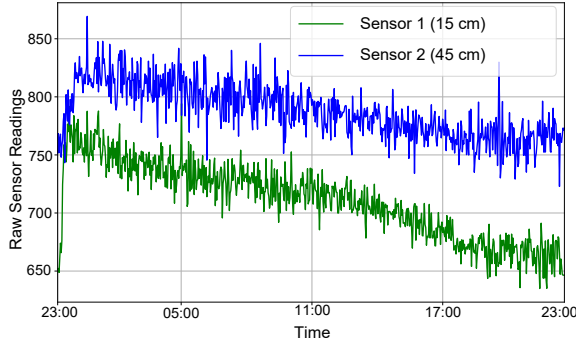


Figure 9: Daily Soil Moisture Readings.

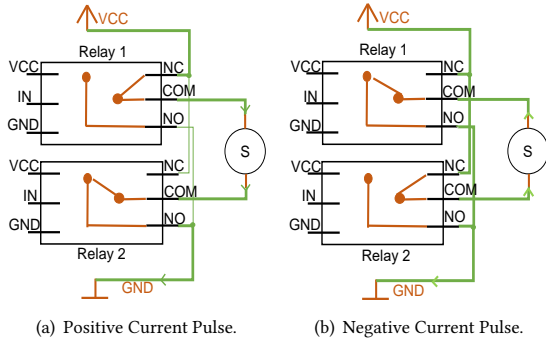


Figure 10: On and off Circuit Diagram for Latching Solenoid.

Sensors: It consists of several moisture sensors for different depths. The moisture sensors vary in their sensitivity and their volume of soil measured. Each moisture sensor for 12-inch depth provides accurate quantitative soil moisture assessment following the Almond Board Irrigation Improvement Continuum [6]. We assign 2 moisture sensors for each *DRLIC* node since the depth of root zone of the almonds in our testbed is 24 inches.

A key feature of the *DRLIC* node is the ability to measure the volumetric water content in the surrounding soil. We opted to purchase research-quality Decagon EC-5 sensors³, with a reported accuracy of $\pm 3\%$. Raw sensor readings collected over a period of one day with a high sampling frequency can be seen in Figure 9. The sensors report the dielectric constant of the soil, which is an electrical property highly dependent on the volumetric water content (VWC).

$$\varphi(m^3/m^3) = 9.92 * 10^{-4} * raw_reading - 0.45 \quad (17)$$

A linear calibration Function 17 above provided by the sensor manufacturer is used to convert the raw readings to VWC. The range of φ is between 0% and 100%. φ of saturated soils is generally 40% to 60% depending on the soil type.

Actuator: It consists of a latching solenoid with two relays. A standard solenoid requires constant power to allow water to flow, making it a poor choice for a battery-powered system. The nine-volt performance all-purpose alkaline batteries from Amazon can only continue to power the standard 12V DC solenoid for 8 hours. To

³Decagon devices. <http://www.decagon.com/products/soils/>

Table 4: Hyperparameters

RL Parameters	Value	General Parameters	Value
Learning_rate	0.01	Iteration	1000
Discount_factor	0.99	Number_neurons	256
Number_layers	2	Clip_parameter	0.3
Minibatches	128	Number_workers	2

extend *DRLIC* node lifetime, we chose to use a latching solenoid for micro-sprinkler actuation, requiring only a 25ms pulse of positive (to open) or negative (to close) voltage. The h-bridge is usually used to produce a bi-directional current to control the latching solenoid [32]. However, it needs a special design to meet different voltages requirements for the ESP32 and latching solenoid.

In order to control the latching solenoid, we design a circuit diagram using two relays to operate with a very little connection overhead. A relay is an electrically operated switch. Figure 10 shows the turn-on and off circuit diagram for latching solenoid. When both the relays are off, there is no current going through the solenoid (S). Initially, both the relays are in a normally closed (NC) position. To turn the solenoid on, Relay 1 is switched from NC to normally open(NO) for 25ms, providing the positive current pulse through the solenoid. The current path shown in Figure 10(a) is: VCC -> NC₁ -> COM₁ -> S -> COM₂ -> NO₂ -> GND. To turn the solenoid off, Relay 2 is switched from NC to NO for 25ms, de-latching the solenoid to the closed position. The current path shown in Figure 10(b) is: VCC -> NC₂ -> COM₂ -> S -> COM₁ -> NO₁ -> GND. To prevent over-irrigation in the event of a power failure, we have the power supply module to continuously provide the power.

Power Supply: Power supply consisted of a 5v, 1.2W solar panel for energy-harvesting and a 18650 Lithium Li-ion battery with a capacity of 3.7V 3000 MAH for energy storage. The TP4056 lithium battery charger module comes with circuit protection and prevents battery over-voltage and reverse polarity connection. All sensors (1 ESP32, 2 moisture sensors, 2 relays and 1 latching solenoid) are powered with this power supply module. It can provide continuous power to prevent over-irrigation in the event of a power failure for the actuator module.

Transmission Module: Transmission includes uplink and downlink. In the uplink path, the moisture sensor readings from the field are sampled by the ESP32, a low-cost, low-power system on a chip (SoC) series with Wi-Fi capability. The readings are then sent from ESP32 to the base station as input for the optimal control. In downlink path, the control command calculated by the DRL agent will be routed to all ESP32 to turn on or off the solenoids.

5 IMPLEMENTATION

In this section, we illustrate in detail the implementation of *DRLIC* and tuning hyper-parameters.

***DRLIC* Implementation Details.** We implement the *DRLIC* system in Python, leveraging widely available open-source frameworks like Pandas, Scikit-learn, and Numpy. The control scheme for *DRLIC* is implemented using RLLib [33], a scalable reinforcement learning framework that supports TensorFlow, TensorFlow Eager, and

PyTorch. RLlib provides a range of customizable options for the training process of the *DRLIC* system, including target environment modeling, neural network modeling, action set building and distribution, and optimal policy learning. For our implementation of *DRLIC*, we collected 10 years of weather data (2010-2020) and used 9 years for training and 1 year for testing. We employed the Adam optimizer with a learning rate of 0.01 for gradient-based optimization and set the discount factor to 0.99. The neural network model features 2 hidden layers with 256 neurons each. The local server used for training and running *DRLIC* is a 64-bit quad-core Intel Core i5-7400 CPU at 3.00 GHz running Ubuntu 18.04.

Training Details and Tuning Hyper-parameters. The performance of the *DRLIC* agent is highly dependent on the values chosen for its hyperparameters. However, there is no straightforward approach that guarantees a specific value will improve the total reward obtained by the system. To optimize the *DRLIC* agent’s hyperparameters and improve its performance, we employ a tuning approach that involves optimizing parameters such as λ , μ associated with rewards and penalties, and learning rates. Specifically, we use a grid search approach that allows us to specify a range of values to be considered for each hyperparameter. The grid search process constructs and evaluates the model using every possible combination of hyperparameters. To evaluate each learned model, we employ cross-validation. This tuning approach allows us to identify the best hyperparameter configuration for the *DRLIC* agent, ensuring optimal *DRLIC* system performance.

6 EVALUATION

In this section, we evaluate the performance of *DRLIC* in the field. We evaluate *DRLIC* system for 15 days in the real world.

6.1 Experiment Setting

6.1.1 Baseline Strategy: We compare *DRLIC* to two state-of-the-art irrigation control schemes introduced in Section 7.

ET-Based Irrigation Control [6]. To implement an ET-based controller, we query a local weather station for the previous day’s ET loss. To compensate for the loss, we use the sprinkler’s irrigation rate provided by its dataset to calculate how long the system should be activated for irrigation.

Sensor-based Irrigation Control [7]. The sensor-based controller has two thresholds, the lower and upper soil water content levels. The first is set at 4.96 inches, 10% higher than MAD to avoid the under irrigation occurring prior to the wetting front arriving at the sensor depth. The latter is set to 6.97 inches, 5% below FC to allow for some rainfall storage. We carefully set these two thresholds based on the soil environment of our testbed.

6.1.2 Performance Metrics. We evaluate the performance of *DRLIC* and two baseline systems in terms of two performance metrics.

Quality of Service. Although the irrigation system has no control over solar exposure and soil nutrients, it has direct control over the moisture levels in the soil. For this reason, our primary metric for irrigation quality is the system’s ability to maintain soil moisture above this MAD threshold at all times at all of our measured locations. By doing so, we are guaranteeing that the plant has sufficient moisture to be healthy and no production loss. In this paper, we call this the quality of service of the irrigation system.

Water Consumption. As each sprinkler uses a water supply and we directly control the times at which each micro-sprinkler is active, we can monitor the amount of water consumed by these three systems at all times to determine the efficiency of each system. Thus another metric is the water consumption, which we would like to minimize subject to the quality of service constraints.

6.1.3 Experiments in our Testbed. We validate the *DRLIC* system with baselines in real-world deployment in terms of plant health and water consumption for 15 days. In the case study, we have six almond trees in our testbed as shown in Figure 8. *DRLIC*, sensor-based control and ET-based control are used to irrigate the upper, middle and lower two trees separately since there is no runoff between trees in our testbed. To allow three irrigation systems to operate independently, Every micro-sprinkler is controlled by a *DRLIC* node. In this way, the only difference among the three systems is the schedules sent to the nodes.

6.2 Experiment Results

6.2.1 Quality of Service. Irrigation systems are installed to maintain almond health with no production loss. Figure 11(a), 11(b), and 11(c) shows the daily soil water content in the field for ET-based control, Sensor-based control and *DRLIC*. The black horizontal line shows the MAD level. If soil water content is below this line, tree health will be impacted. We can see that *DRLIC* and ET system can maintain the soil water content above MAD threshold during the 15 days deployment and thus meet the requirement of almond health. However, the trees irrigated by Sensor-based method are in an under-irrigation period of 18 hours for four days (day 1, 4, 7 and 9) since the soil water content of Sensor-based method is lower than the MAD. The reason is that the moisture level of previous day is close but not reached to MAD, so the sensor-based method will not irrigate even though the moisture level is in an under-irrigation trend. *DRLIC* system can irrigate what the trees need based on the learned model about the water changes in the soil and maintain the soil water content close to MAD level.

All three underlying irrigation systems begin with enough water content on the first day. We see that the soil water contents of the two trees in ET control system are much above the FC threshold. In our deployment of *DRLIC* against the ET control strategy in Figure 11(a), we see that soil water content for these two trees is different and much higher than the MAD level. This emphasizes the limitations of ET and the core of our work. The irrigated regions don’t receive moisture the same way, and most of the time, the ET-based controller irrigates more water than the plant needs.

6.2.2 Water Consumption. When a decision must be made to switch to a new almond irrigation control system, a primary concern is the efficiency of the proposed system. The system’s ability to return its investment based on increased efficiency will often dictate the acceptance of the technology. In addition, the environmental benefits of reduced freshwater consumption are clear and help promote system adoption.

In our experimental setup, the water source provided by each micro-sprinkler is pressure-regulated to the industry standard, 30

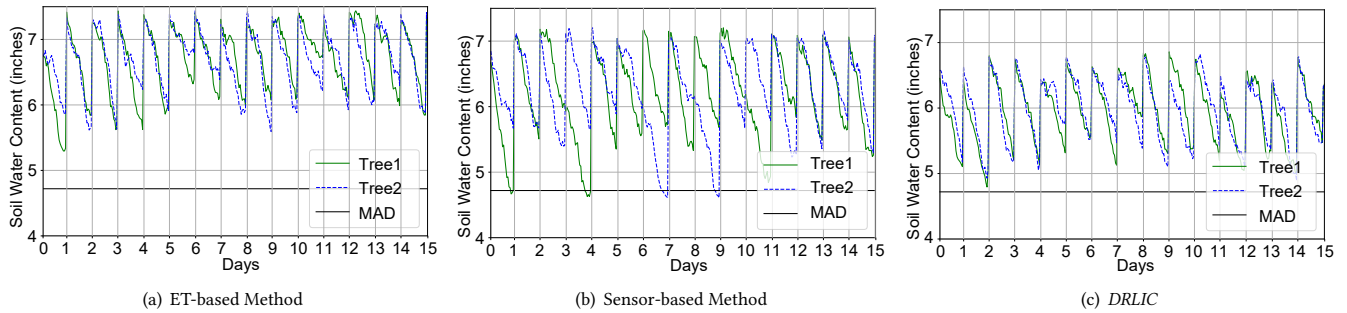


Figure 11: Daily Soil Water Content of Different Irrigation Methods (15 Days).

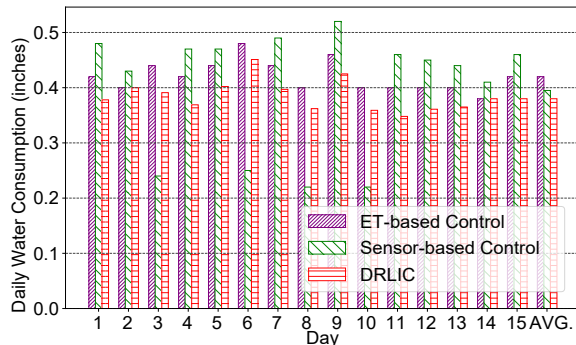


Figure 12: Daily Water Consumption.

psi. Each micro-sprinkler head distributing water uses a clearly-defined amount of water per unit time, as described in the almond irrigation manual [6]. By tracking exactly when each micro-sprinkler is actuated by the system, we can determine very accurately how much water has been consumed.

Figure 12 shows the daily irrigation amount of two trees actuated by ET-based control, sensor-based control and *DRLIC* in a 15 days’ deployment experiment. From this figure, we can see that *DRLIC* can save an average 9.52% and 3.79% of the water compared with ET-based and Sensor-based control during 15 days deployment experiment. ET-based control is a centralized control method to irrigate all almond trees without considering their specific need. Sensor-based control is water-efficient by monitoring the moisture and irrigating when the moisture level is lower than the MAD level. However, the thresholds are site-specific and not optimal. *DRLIC* can learn optimal irrigation control by interacting with the local weather and soil water dynamic environment.

6.3 Simulation Results

In this section, we discuss the simulation results of *DRLIC* and two baselines for a whole growing season.

6.3.1 Quality of Service. Figure 13 shows daily soil water content for ET-based control, Sensor-based control and *DRLIC* in the simulation. The black horizontal line shows the MAD level. We can see that all four control methods can maintain the soil water content above the MAD level and thus meet the requirement of the almond health. Especially on days 2, 5, 24 of March and 16 and 18 of May, we can see that all water content of each tree for all four control systems are the same. The reason is that all of those days have big rainfall

and thus make the soil reach the field capacity. In our deployment of *DRLIC* against the ET-based control strategy in Figure 13(a), we see that soil water content for these two trees in the control system is different and much higher than the MAD level. The sensor-based control maintains two moisture levels, the lower level to start and a higher level to stop irrigation. From Figure 13(b), we can see that even though we carefully set these two values for each tree, there are still 43 days the soil water content is slightly under the MAD level which may affect the almond production. Overall, *DRLIC*_{MAD} and *DRLIC* system (Figure 13(c)) can maintain the health of all two trees in a uniform irrigation way in the growing season.

6.3.2 Water Consumption. Figure 14 shows the monthly water consumption by ET-based system, Sensor-based system, and *DRLIC* system from March to October. We can see that *DRLIC* consume less water for each month compared to ET-based and Sensor-based systems. We can also see that the irrigation amount increases and then decreases for all systems. There are two reasons. First, spring rains stop and the weather heats up. Second, the almonds and the trees go through 3 stages in their annual lifecycle, including dormancy during winter, the stunning bloom in March, “growing up” through the spring, and “cracking open” in summer. The year finishes up with harvest spanning from mid-August to October. So in the summer, water consumption is higher than other seasons. Overall, *DRLIC* system can save 10.21% and 3.93% of water than ET system and Sensor-based system for the whole growing season. California’s 2019 almond acreage is estimated at 1,530,000 acres, and almond irrigation is estimated to consume roughly 195.26 billion gallons per year [4]. With *DRLIC* system, 19.94 and 7.67 billion gallons of water can be saved per year.

6.4 Effect of our Safe Irrigation Mechanism.

In the 15 days’ deployment, we find that there are two days (Day 2 and 14 in Figure 11(c)) *DRLIC* triggers the ET-control method. This can also be validated from Figure 12, we can find the water consumption of ET method and *DRLIC* on days 2 and 14 are the same. We check the weather data to understand the reason and find that the wind speeds of days 2 and 14 are 7.2 and 11.9 mph respectively which is much higher than the average 2.8 mph of the other 13 days.

We now run *DRLIC* with and without safe mechanism for a whole growing season in simulation, labeled as Robust-RL and RL-only, respectively. Figure 13(c) and 15 show the daily soil water

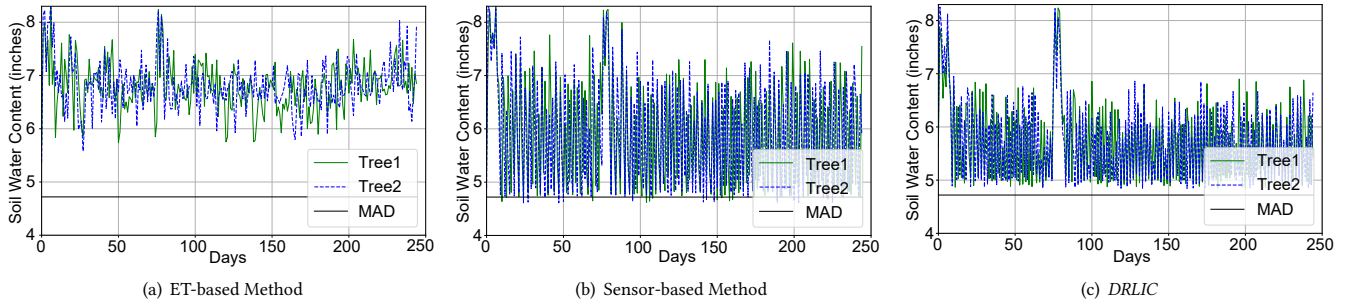


Figure 13: Daily Soil Water Content of Different Irrigation Methods.

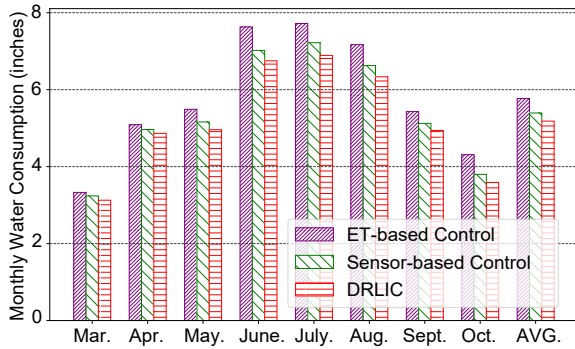


Figure 14: Monthly Water Consumption.

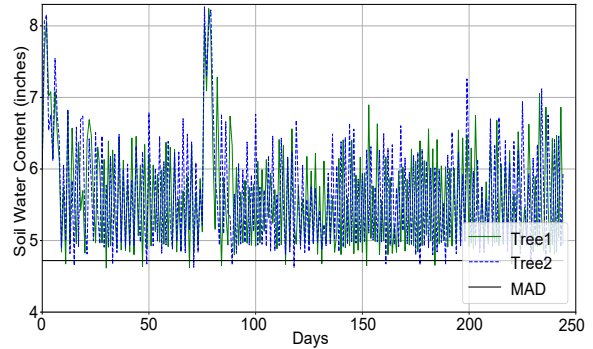


Figure 15: Daily Soil Water Content (w/o Safe Mechanism).

content of Robust-RL and RL-only for a same growing season 2020, respectively. From the almond’s perspective, Robust-RL maintains health with 0 days below the MAD level. The RL-only irrigation method has 21 days below the MAD level. The reason is that the RL models trained from past weather data “misbehave” on the test weather data. while it may be possible to train on changing weather to obtain a robust policy, no offline training can ever cover all possible weather changes. The RL agent with safe mechanism from *DRLIC*, however, is robust to weather changes because the safety condition detector will detect the dangerous actions from RL agent and the ET system will take control.

6.5 Effect of proposed Reward.

In this section, we discuss the simulation results of *DRLIC* with different rewards for a whole growing season (March 1st to October 31st, 246 days).

In order to minimize water consumption while not affecting plant health, we consider three situations in the reward. 1) The soil water content (V_i) is higher than the FC (V_{fc}) level. 2) V_i is between V_{fc} and V_{mad} . 3) V_i is lower than V_{mad} . Only in the second situation, the plants are in good health. To evaluate our reward function, we compare it with a simple reward ($DRLIC_{MAD}$) that only maintains V_i above V_{mad} . It is commonly used in the sensor-based method [7]. The reward is defined as: $R = -\sum_{i=1}^N \lambda_3 * (V_{mad} - V_i) + \mu_3 * a_i, V_i < V_{mad}$. This function gives more penalty to plant health when V_i is lower than V_{mad} since plants’ health is significantly impacted. All the parameters are the same in Section 3.3.3.

Figure 19 shows the water consumption of *DRLIC* with our proposed reward (*DRLIC*) and the simple reward (*DRLIC_MAD*). *DRLIC* can save 2.04% more water than *DRLIC_MAD*, as the latter does not consider the case when V_i is higher than V_{mad} . *DRLIC* considers two more situations by giving different penalties to plants’ health and water consumption. The first case is over-irrigation. The water consumption is too high. Therefore, the penalty for water consumption is higher than plant health. In the second case, the plants are in good health. *DRLIC* strives to maintain the V_i close to V_{mad} to save more water.

6.6 DRLIC Policy Convergence.

Figure 16 shows the RL training process and the policy converges around the 500th training iteration. We define the length of an episode as 30 days. We randomly vary the soil water content for each tree between the FC (7.08 inches) and MAD (4.72 inches) at the beginning of each episode. By doing so, the policy is exposed to different soil water content conditions and learns to avoid water depletion than the MAD level during training. At the beginning of the experiment, the RL policy receives a larger negative reward as it does not know a valid sequence of actions that maximize the reward. The policy converges at the 500th training iteration. The whole training (i.e. 1000 training iterations) takes ~ 4 hours using a 64-bit quad-core Intel Core i5-7400 CPU at 3.00 GHz.

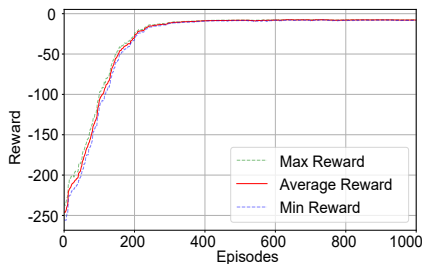


Figure 16: Reinforcement Learning Policy Convergence.

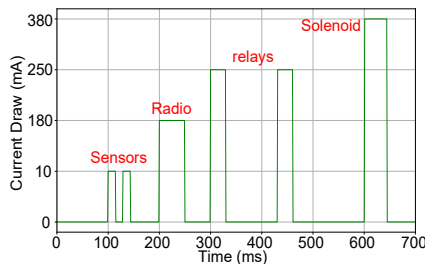


Figure 17: Energy Profile for Different Kinds of Sensors.

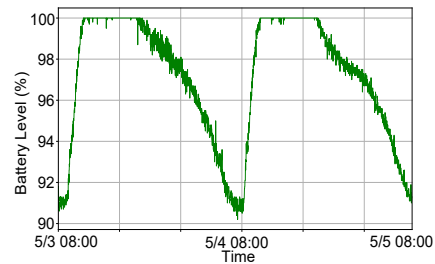


Figure 18: Battery Charging and Discharging Cycle.

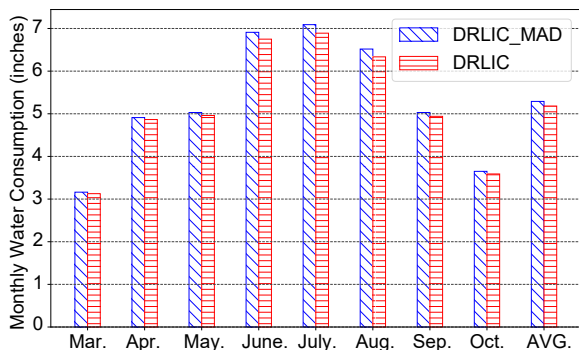


Figure 19: Water Consumption for *DRLIC* with Different Reward

Table 5: Micro-sprinkler Node Manufacture Cost.

Component	Price	Component	Price
Moisture Sensor x 2	\$250	ESP32	\$6.5
18650 Li-ion battery	\$3	Solar Panel	\$4.3
Latching Solenoid	\$4	Switch Relay x 2	\$5
Waterproof Enclosure	\$12	Maintenance Fee	\$10
		Total	\$294.8

6.7 Energy Consumption of Sensor Nodes

From a wireless sensor network standpoint, the ability of a system to operate for a long period of time without user intervention is fundamental. *DRLIC* nodes are no different, especially if they are meant to be put on the ground. For this reason, our hardware and software were designed to consume as little energy as possible. *DRLIC* nodes were fitted with a latching solenoid, allowing the flow of water to be turned on or off with a short pulse of power, rather than a constant supply. For additional energy savings, the radio in each node is duty-cycled, activating for only a 10 second period every 1 minute. We need this high data frequency, the reason is that the base station can send an off command to *DRLIC* with a minute granularity. In our devices, the four peripherals that consume significant energy are the two moisture sensors, solenoid, two relays and radio. To meet this energy, we design an energy harvesting mechanism by leveraging one 5/6 V 1.2 W solar panel.

Figure 17 shows the energy consumption for different sensors. Each moisture sensor sample requires 10 mA of power for 10 ms, and each flip of the latching solenoid requires 380 mA of power for 30ms. The ESP32 radio requires 180 mA of power for 50ms when

in transmitting mode. The relay requires 250 mA for 20 ms for switching on or off. In our system, to ensure we don't cut power too early, we add a safety band of 50% on the timing on both of these devices, triggering for 15 ms and 45 ms for the sensor and solenoid, respectively. Overall, the solar-harvest mechanism can meet the daily requirement of all the sensors in *DRLIC* node.

Figure 18 shows the two days' energy charging and discharging process. After a night discharge, the 18650 battery level is increasing at 9:15 am on May 3rd. It usually takes 2 hours to fully charge the battery (9:15 - 11:35 am). The battery level will keep 100% from 11:35 am to 18:45 pm, the energy harvested from solar can meet the energy requirement of all sensors in *DRLIC* node. The battery will discharge from 100% at 18:45 pm of May 3rd to the 90.7% at 8:45 am of May 4th. Then the whole energy charging and discharging process repeat. The lowest battery level is an average of 90%. In the 2 week's deployment, we find that even on a cloudy day, the battery can also be charged and will take one more hour to be fully charged.

6.8 Return on Investment

A primary concern to purchasing or upgrading an irrigation control system is the return on investment, i.e., how long does it take to save enough money from water consumption to cover the cost of the new irrigation system. To calculate the return on investment of *DRLIC*, we take into account the initial investment cost of the *DRLIC* system and the money saved from the less water consumption provided by our increased irrigation efficiency.

We first calculate the cost to develop a single *DRLIC* node. All the components of a *DRLIC* node can be found in a consumer electronics store and a home improvement store. Table 5 lists the cost of all components. In total, a *DRLIC* sensing and actuation node costs \$294.8. A large portion of the budget is the cost of two soil moisture sensors. We use two expensive soil moisture sensors that provide accurate measurement and a long lifetime.

The factors that mostly influence the payback of our system are water price and water volume saved by *DRLIC*. Water price varies considerably in different irrigation district and over time. This study assumed 100% groundwater usage and availability. Each tree costs \$11.3 for irrigation water per month. Based on our experiment results, *DRLIC* can save 9.52% of water expense per month, corresponding to \$1.08. Normally, almond orchards have 100 trees per acre. As a result, *DRLIC* can save \$108 per month. Take a 60-acre almond orchard with 10 irrigation regions as an example. Each

irrigation region is six acres. *DRLIC* can save \$648 in each irrigation region per month.

In each irrigation region, we need to deploy one *DRLIC* node, which costs \$294.8. The other irrigation components will use the existing infrastructure, such as the pipelines and micro-sprinklers under each tree. The cost of upgrading the existing irrigation system with our irrigation control system is \$294.8 for one irrigation region in an orchard. Every month, our system can save \$648. Therefore, it only needs half a month for our irrigation system to return the investment.

7 RELATED WORK

ET-Based Irrigation Control. As the weather is a primary water source or sinks in an irrigated space, systems have been developed to use weather as input for control. The simplest of these systems use standard fixed-schedule irrigation, but allow a precipitation sensor to override control to save water during rain [34]. The more complicated systems, now the industry standard, use evapotranspiration (ET), an estimate of the amount of water lost to evaporation and plant transpiration to do efficient water-loss replacement [35, 36]. Some providers boast an average 30% reduction in water consumption, but as with all industry irrigation systems, ET-based systems are limited by centralized control, and can not provide site-specific irrigation, reducing potential system efficiency and quality of control.

Sensor-based Irrigation Control. With the introduction of more accurate and efficient soil moisture sensors, work has been done to create irrigation controllers that react directly to moisture levels in the soil [7, 37, 38]. Moisture sensors buried in the root zone of trees accurately measure the moisture level in the soil and transmit this data to the controller. The controller then adjusts the pre-programmed watering schedule as needed. There are two types of soil moisture sensor-based systems: 1) Suspended cycle irrigation systems. Suspended cycle irrigation systems use traditional timed controllers and automated watering schedules, with start times and duration. The difference is that the system will stop the next scheduled irrigation cycle when there is enough moisture in the soil. 2) Water on-demand irrigation requires no programming of irrigation duration (only start times to water). This type maintains two soil moisture thresholds. The lower one to initiate watering, and the upper one to terminate watering [7]. However, without a model of the way water is lost, these thresholds are usually set based on experience and are not optimal.

Model-based Irrigation Control. In [32, 39], a mechanistic PDE model of moisture movement within irrigated space is built. Using this model, an optimal watering schedule can be found to maintain a proper moisture level. However, the PDE model is not updated over time and future weather prediction is not taken into account. To tackle these two limitations, the same authors further improve the control system in [14, 40]. The PDE model is eschewed in favor of an adaptive approach that involves models trained from sensor data. Long-term and short-term models are developed to describe the relationship of runoff between sprinklers in the movement of water through the soil.

As indicated by the authors [14, 40], their system is designed for turf irrigation, and it is unlikely to provide benefit in shrubbery or

tree irrigation. First, the turf soil moisture is affected by water runoff on soil surface and the overlapping coverage of sprinklers. The models in [14, 40] are focused on capturing the relationship of runoff between sprinklers. For tree irrigation, however, there is little runoff due to the tree space. The soil moisture model for tree irrigation needs to consider the soil-water relationship under different depths. Second, as shown in [41], the decay of volumetric water content derived from the long-term model of [14] was shown to be much quicker than the real-world scenarios. It is bound to irrigate lightly and frequently, which has been found to be inefficient [42].

DRL-based Control. DRL has been applied in many applications, such as network planning [17], cellular data analytics [18], sensor energy management [43], mobile app prediction [44, 45] and building energy optimization [46, 47]. In particular, DRL techniques have demonstrated the potential optimal irrigation controls. [48] proposed a reinforcement learning-based irrigation control system. The basic idea is to use a reinforcement learning algorithm to perform both irrigation planning and scheduling. Two neural networks (NNs) are also introduced to predict DSSAT (Decision Support System for Agrotechnology Transfer) [49] simulation results. DSSAT is the defacto standard model for crop growth. One NN inputs irrigation and weather information and predicts total soil water content, while the other NN predicts crop yield, given the daily total soil water content for an entire crop season. The prediction of crop yield is then used as the training data to train the reinforcement learning model. This approach can achieve relatively precise irrigation and allows full automation of the irrigation process. However, it is restricted to a small state space and is difficult to scale to large problems. Therefore, accurate representation of the actual irrigation context is difficult, leading to loss of important information that is needed for optimizing irrigation decisions. To solve this small state space problem, a deep reinforcement learning-based irrigation scheduling approach [50] is introduced for optimizing irrigation applications in terms of net return. This approach determines the amount of irrigation for each zone at each time step, taking soil moisture, evapotranspiration, precipitation probability, and crop growth stage into consideration. Compared to the previous approach using traditional reinforcement learning, it can handle a much greater state space and a greater number of irrigation choices. However, this control method is still central-valve control and thus affects the production performance.

TestBed TestBeds are widely used to study the precision irrigation. There are several existing platforms with features required for irrigation control [51–54]. The Farmbot is a CNC style mechanism that consists of a plot for vegetables and a modular set of interchangeable tools [51, 52]. The tools can execute a variety of tasks including soil moisture sensing, RGB imaging, planting, weeding, and irrigating. The basic assembly kit is priced at USD \$2595. [53, 54] presented RAPIDMOLT, a modular, open-source testbed that enables real-time, fine-grained data collection and irrigation actuation. RAPIDMOLT costs USD \$600 and has floor space of $0.37 m^2$. The functionality of the platform is evaluated by measuring the correlation between plant growth (Leaf Area Index) and water stress (Crop Water Stress Index) with irrigation volume. Both these two TestBeds are used for vegetables, not for trees with much deep soil and large scale.

8 CONCLUSIONS

We present *DRLIC*, a DRL-based irrigation system that generates optimal irrigation control commands according to current soil water content, current weather data and forecasted weather information. A set of techniques have been developed, including our customized design of DRL states and reward for optimal irrigation, a validated soil moisture simulator for fast DRL training, and a safe irrigation module. We design *DRLIC* irrigation node and build a testbed of six almond trees. Extensive experiments in real-world and simulation show the efficiency of *DRLIC* system.

9 ACKNOWLEDGMENTS

We would like to thank our anonymous shepherd and reviewers for their constructive comments. We also thank Danny Royer for helping us set up the testbed. This research is partially supported by the National Science Foundation under grants #CCF- 2008837, a 2020 Seed Fund Award from CITRIS and the Banatao Institute at the University of California, and a 2022 Faculty Research Award through the Academic Senate Faculty Research Program at the University of California, Merced.

REFERENCES

- [1] Field capacity. <https://nrcca.cals.cornell.edu/soil/CA2/CA0212.1-3.php>.
- [2] R Troy Peters, Kefyalew G Desta, and Leigh Nelson. Practical use of soil moisture sensors and their data for irrigation scheduling. 2013.
- [3] Soil quality indicators. https://www.nrcs.usda.gov/Internet/FSE_DOCUMENTS/nrcs142p2_053288.pdf.
- [4] Julian Fulton, Michael Norton, and Fraser Shilling. Water-indexed benefits and impacts of californian almonds. *Ecological indicators*, 96:711–717, 2019.
- [5] 2018 Almond Board of California. Water footprint for almonds. https://almonds.com/sites/default/files/2020-05/Water_footprint_plus_almonds.pdf.
- [6] Almond Board of California. Almond irrigation improvement continuum. <https://www.almonds.com/sites/default/files/2020-02/Almond-Irrigation-Improvement-Continuum.pdf>.
- [7] GL Grabow, IE Ghali, RL Huffman, et al. Water application efficiency and adequacy of et-based and soil moisture-based irrigation controllers for turfgrass irrigation. *Journal of irrigation and drainage engineering*, 2013.
- [8] Xianzhong Ding and Wan Du. Smart irrigation control using deep reinforcement learning. In *ACM/IEEE IPSN*, 2022.
- [9] Yenny Fernanda Urrego-Pereira, Antonio Martinez-Cob, and Jose Caverro. Relevance of sprinkler irrigation time and water losses on maize yield. *Agronomy Journal*, 2013.
- [10] Dilini Delgoda, Hector Malano, Syed K Saleem, and Malka N Halgamuge. Irrigation control based on model predictive control (mpc): Formulation of theory and validation using weather forecast data and aquacrop model. *Environmental Modelling & Software*, 2016.
- [11] Camilo Lozoya, Carlos Mendoza, Leonardo Mejía, Jesús Quintana, Gilberto Mendoza, Manuel Bustillos, Octavio Arras, and Luis Solís. Model predictive control for closed-loop irrigation. *IFAC Proceedings Volumes*, 2014.
- [12] Bruno Silva Ursulino, Suzana Maria Gico Lima Montenegro, Artur Paiva Coutinho, et al. Modelling soil water dynamics from soil hydraulic parameters estimated by an alternative method in a tropical experimental basin. *Water*, 2019.
- [13] California department of water resources. <https://www.cimis.water.ca.gov/>.
- [14] Daniel A Winkler, Miguel Á Carreira-Perpiñán, and Alberto E Cerpa. Plug-and-play irrigation control at scale. In *ACM/IEEE IPSN*, 2018.
- [15] Shmulik P Friedman. Is the crop evapotranspiration rate a good surrogate for the recommended irrigation rate? *Irrigation and Drainage*, 2023.
- [16] Haoyu Niu, Dong Wang, and YangQuan Chen. Estimating actual crop evapotranspiration using deep stochastic configuration networks model and uav-based crop coefficients in a pomegranate orchard. In *Autonomous Air and Ground Sensing Systems for Agricultural Optimization and Phenotyping V*. International Society for Optics and Photonics, 2020.
- [17] Hang Zhu, Varun Gupta, Satyajeet Singh Ahuja, Yuandong Tian, Ying Zhang, and Xin Jin. Network planning with deep reinforcement learning. In *Proceedings of the 2021 ACM SIGCOMM 2021 Conference*, 2021.
- [18] Zhihao Shen, Wan Du, Xi Zhao, and Jianhua Zou. Dmm: fast map matching for cellular data. In *Proceedings of the 26th annual international conference on mobile computing and networking*, 2020.
- [19] Miaomiao Liu, Xianzhong Ding, and Wan Du. Continuous, real-time object detection on mobile devices without offloading. In *2020 IEEE 40th International*

- Conference on Distributed Computing Systems (ICDCS)*, pages 976–986. IEEE, 2020.
- [20] Devanshu Kumar, Xianzhong Ding, Wan Du, and Alberto Cerpa. Building sensor fault detection and diagnostic system. In *Proceedings of the 8th ACM International Conference on Systems for Energy-Efficient Buildings, Cities, and Transportation*, pages 357–360, 2021.
- [21] Xianzhong Ding, Wan Du, and Alberto Cerpa. Octopus: Deep reinforcement learning for holistic smart building control. In *ACM BuildSys*, 2019.
- [22] Xianzhong Ding, Wan Du, and Alberto E Cerpa. Mb2c: Model-based deep reinforcement learning for multi-zone building control. In *Proceedings of the 7th ACM international conference on systems for energy-efficient buildings, cities, and transportation*, 2020.
- [23] Volodymyr Mnih, Koray Kavukcuoglu, David Silver, Alex Graves, Ioannis Antonoglou, Daan Wierstra, and Martin Riedmiller. Playing atari with deep reinforcement learning. *arXiv preprint arXiv:1312.5602*, 2013.
- [24] John Schulman, Filip Wolski, Prafulla Dhariwal, Alec Radford, and Oleg Klimov. Proximal policy optimization algorithms. *arXiv preprint arXiv:1707.06347*, 2017.
- [25] Artem Molchanov, Tao Chen, Wolfgang Hönig, James A Preiss, Nora Ayanian, and Gaurav S Sukhatme. Sim-to-(multi)-real: Transfer of low-level robust control policies to multiple quadrotors. In *IEEE IROS*, 2019.
- [26] Christopher Berner, Greg Brockman, Brooke Chan, et al. Dota 2 with large scale deep reinforcement learning. *arXiv preprint arXiv:1912.06680*, 2019.
- [27] Su Ki Ooi, Iven Mareels, Nicola Cooley, Greg Dunn, and Gavin Thoms. A systems engineering approach to viticulture on-farm irrigation. *IFAC Proceedings Volumes*, 2008.
- [28] Guotao Cui and Jianting Zhu. Infiltration model based on traveling characteristics of wetting front. *Soil Science Society of America Journal*, 82(1):45–55, 2018.
- [29] Guotao Cui and Jianting Zhu. Prediction of unsaturated flow and water backfill during infiltration in layered soils. *Journal of Hydrology*, 557:509–521, 2018.
- [30] Dilini Delgoda, Syed K Saleem, Hector Malano, and Malka N Halgamuge. Root zone soil moisture prediction models based on system identification: Formulation of the theory and validation using field and aquacrop data. *Agricultural Water Management*, 2016.
- [31] George H Hargreaves and Zohrab A Samani. Reference crop evapotranspiration from temperature. *Applied engineering in agriculture*, 1(2):96–99, 1985.
- [32] Daniel A Winkler, Robert Wang, Francois Blanchette, Miguel Carreira-Perpiñán, and Alberto E Cerpa. Magic: Model-based actuation for ground irrigation control. In *ACM/IEEE IPSN*, 2016.
- [33] Eric Liang, Richard Liaw, Robert Nishihara, Philipp Moritz, Roy Fox, Ken Goldberg, Joseph Gonzalez, Michael Jordan, and Ion Stoica. Rllib: Abstractions for distributed reinforcement learning. In *ICML. PMLR*, 2018.
- [34] Hunter. Hunter rain-click rain detection. hunterindustries.com/irrigation-product/sensors/rain-click/.
- [35] Richard G Allen, Luis S Pereira, Dirk Raes, Martin Smith, et al. Crop evapotranspiration-guidelines for computing crop water requirements-fao irrigation and drainage paper 56. *Fao, Rome*, 1998.
- [36] Marvin Eli Jensen, Robert D Burman, and Rick G Allen. Evapotranspiration and irrigation water requirements. ASCE, 1990.
- [37] Ugmo irrigation. <http://www.ugmo.com/>.
- [38] Yunseop Kim, Robert G Evans, and William M Iversen. Remote sensing and control of an irrigation system using a distributed wireless sensor network. *IEEE TIM*, 2008.
- [39] Daniel A Winkler, Robert Wang, Francois Blanchette, Miguel A Carreira-Perpinan, and Alberto E Cerpa. Dictum: Distributed irrigation actuation with turf humidity modeling. *ACM Transactions on Sensor Networks (TOSN)*, 15(4):1–33, 2019.
- [40] Daniel A Winkler, Miguel Á Carreira-Perpiñán, and Alberto E Cerpa. Optics: Optimizing irrigation control at scale. *ACM Transactions on Sensor Networks (TOSN)*, 16(3):1–38, 2020.
- [41] Akshay Murthy, Curtis Green, Radu Stoleru, Suman Bhunia, Charles Swanson, and Theodora Chaspari. Machine learning-based irrigation control optimization. In *ACM BuildSys*, 2019.
- [42] Light and frequent irrigation. <https://www.usga.org/course-care/water-resource-center/our-experts-explain--water/is-it-better-to-irrigate-light-and-frequent-or-deep-and-infrequent.html>.
- [43] Francesco Fraternali, Bharathan Balaji, Dhiman Sengupta, Dezhi Hong, and Rajesh K Gupta. Ember: energy management of batteryless event detection sensors with deep reinforcement learning. In *ACM SenSys*, 2020.
- [44] Zhihao Shen, Kang Yang, Zhao Xi, Jianhua Zou, and Wan Du. Deepapp: a deep reinforcement learning framework for mobile application usage prediction. *IEEE Transactions on Mobile Computing*, 2021.
- [45] Kang Yang, Xi Zhao, Jianhua Zou, and Wan Du. Atp: A mobile app prediction system based on deep marked temporal point processes. In *IEEE DCOS*, 2021.
- [46] Xianzhong Ding, Alberto Cerpa, and Wan Du. Exploring deep reinforcement learning for holistic smart building control. *arXiv preprint arXiv:2301.11510*, 2023.
- [47] Xianzhong Ding, Alberto Cerpa, and Wan Du. Multi-zone hvac control with model-based deep reinforcement learning. *arXiv preprint arXiv:2302.00725*, 2023.
- [48] Lijia Sun, Yanxiang Yang, Jiang Hu, Dana Porter, Thomas Marek, and Charles Hillyer. Reinforcement learning control for water-efficient agricultural irrigation.

- In *2017 IEEE International Symposium on Parallel and Distributed Processing with Applications and 2017 IEEE International Conference on Ubiquitous Computing and Communications (ISPA/IUCC)*. IEEE, 2017.
- [49] James W Jones, Gerrit Hoogenboom, Cheryl H Porter, Ken J Boote, William D Batchelor, LA Hunt, Paul W Wilkens, Upendra Singh, Arjan J Gijssman, and Joe T Ritchie. The dssat cropping system model. *European journal of agronomy*, 2003.
- [50] Yanxiang Yang, Jiang Hu, Dana Porter, Thomas Marek, Kevin Heflin, and Hongxin Kong. Deep reinforcement learning-based irrigation scheduling. *Transactions of the ASABE*, 2020.
- [51] Open-source cnc farming. Available:<https://farm.bot/>.
- [52] Mohammad Nafe Momin, Ashar Mohd Ansari, Abhijit Balasaheb Kadam, Omkar Preetam Choughule, Umer Salim Bhikan, et al. Design and fabrication of arduino based farm-bot for precision farming. 2019.
- [53] Marius Wiggert, Leela Amladi, Ron Berenstein, Stefano Carpin, Joshua Viers, Stavros Vougioukas, and Ken Goldberg. Rapid-molt: A meso-scale, open-source, low-cost testbed for robot assisted precision irrigation and delivery. In *2019 IEEE 15th International Conference on Automation Science and Engineering (CASE)*. IEEE, 2019.
- [54] Mark Presten and Ken Goldberg. Design and implementation of physical experiments for evaluation of the alphagarden: an autonomous polyculture garden. 2022.